Rare Metal Materials and Engineering
Volume 48, Issue 6, June 2019
Available online at www.rmme.ac.cn

Science Press

Cite this article as: Rare Metal Materials and Engineering, 2019, 48(6): 1785-1790.

ARTICLE

Improved Oxidation Resistance of a CeO_2-modified Aluminide Coating by Low-Temperature Pack Cementation

Tan Xiaoxiao

Shanghai University of Science and Engineering, Shanghai 201620, China

Abstract: CeO_2-free and CeO_2-modified aluminide coatings were prepared by aluminizing pure Ni film and Ni-CeO_2 film on Ni plate at 620 °C, respectively. The effect of the CeO_2 addition on the growth rate and adhesion of the alumina scale at 1000 °C was investigated. The results show that the addition of nanometer CeO_2 in aluminide coating of δ phase delays the formation of a continuous α-Al_2O_3 scale and decreases the growth rate of alumina scale during oxidation. Moreover, the alumina scale adhesion is improved by the addition of nanometer CeO_2 due to the smaller cavities formed at the alumina scale/coating interface compared with the CeO_2-free one.

Key words: aluminide coating; oxidation; pack cementation; reactive element effect (REE)

The pack cementation process as the most mature aluminizing process is widely used to aluminize nickel-base superalloys or steels to improve their oxidation resistance at high temperature[1,2]. The thermally grown α-Al_2O_3 scale at the surface of aluminide coatings can provide effective protection because of its compact structure, low thermal growth kinetics and volatility[3]. However, α-Al_2O_3 with dense hexagonal structure directly forms only during oxidation over 1200 °C, while the transient Al_2O_3 with square structure firstly forms between 800 °C and 1200 °C[4]. Then the transient Al_2O_3 is transformed to α-Al_2O_3 with the prolongation of time. In this temperature range, the transient Al_2O_3 are mainly in γ, δ and θ phases and the thermal stability increases gradually from γ to θ. Compared with α-Al_2O_3, these transient Al_2O_3 are not protective due to the relatively looser structure and higher growth rate. Moreover, the phase transition from transient Al_2O_3 to α-Al_2O_3 accompanied with ~13% volume shrinkage would lead to the cracking of alumina scale, which accordingly causes the breakaway oxidation[5]. Thus, the phase transition process has an important effect on the oxidation resistance of the alumina-forming alloys between 800 °C to 1200 °C. Besides, cracking and spalling occur due to the thermal stress introduced by thermal expansion coefficient mismatch between the alumina scale and the metal substrate during cooling or under thermal cycling, which negatively affects the oxidation resistance and service life of aluminide coatings at high temperature[6-9].

Reactive elements (RE), such as cerium, lanthanum and yttrium, or their oxides can significantly reduce the oxidation rate of the alloy and improve the adhesion of the alumina scale, which is referred to as “reactive element effect” (REE). Subsequently, RE-modified aluminide coatings have been widely applied on superalloys [10-13]. The reported variation of the alumina growth rate between the RE-free and RE-modified alloys has great difference and unobvious regularity, mainly due to the different experimental conditions, RE amounts, alloy types and transition rate from transient Al_2O_3 to stable Al_2O_3[14,15]. The growth of the transient Al_2O_3 (such as θ) is controlled by the outward diffusion of Al ions, forming typical morphology of needle or blade[4, 16]. When RE or their oxides are added, the needle-like or blade-like structure is suppressed[17]. It is generally recognized that the growth of α-Al_2O_3 is controlled by both the outward diffusion of Al ions and the inward diffusion of oxygen ions. Previous results studied by oxygen isotope method show that RE can greatly reduce the outward diffusion rate of Al ions, but have little effect on the inward

Received date: September 06, 2018
Foundation item: National Natural Science Foundation of China (51501109)
Corresponding author: Tan Xiaoxiao, Ph. D., Lecturer, Engineering Training Center and School of Materials Engineering, Shanghai University of Science and Engineering, Shanghai 201620, P. R. China, Tel: 0086-21-67791247, E-mail: xxtan@sues.edu.cn

diffusion of oxygen ions[18]. In the meantime, many researchers have observed the segregation of RE ions at grain boundaries and scale/metal interface by field emission scanning transmission electron microscopy (FESEM) and secondary ion mass spectrometry (SIMS)[17,19]. On basis of the results, it is proposed that RE ions with large radius tend to segregate at grain boundaries or interface, which block the outward diffusion of Al ions, accordingly decreasing the oxidation rate and changing the growth mechanism of the alumina scale.

The formation of large cavities and sulfur segregation at the scale/metal interface are the main reasons for scale detachment. Various models have been presented to explain the effect of RE on the adhesion of alumina scale. For example, it is believed that the added RE oxides could increase the vacancy "sinks" and reduce the size of the interfacial voids[7,20]. It is also recognized that RE addition can bind the S impurities in some way, greatly reducing the sulfur segregation at the interface[21,22]. However, each model has its limitations and the researchers have not yet reached a consensus.

In this investigation, CeO_2-free and CeO_2-modified aluminide coatings were prepared by low-temperature pack cementation process. The effect of the CeO_2 addition on the growth rate and adhesion of the alumina scale at 1000 °C was investigated.

1 Experiment

Specimens with dimensions of 15 mm×10 mm×2 mm were extracted from the as-received pure Ni plate. After being abraded by SiC paper to 800 grit and then ultrasonically cleaned in alcohol and acetone, the specimens were electrodeposited with a Ni-CeO_2 film from a nickel sulfate bath (150 g/L $NiSO_4·6H_2O$, 120 g/L $C_6H_5Na_3O_7·2H_2O$, 12 g/L NaCl, 35 g/L H_3BO_3) loaded with CeO_2 particles. The CeO_2 nanoparticles (15~30 nm) were commercial products from Alfa Aesar. For comparison, a CeO_2-free Ni film was electrodeposited from a similar bath but without CeO_2 loading. Afterward, the deposited specimens were aluminized at 620 °C for 5 h using a conventional halide activate pack-cementation method in a powder mixture of Al (particle size: ~75 μm) + 55 wt% Al_2O_3 (~75 μm) + 5 wt% NH_4Cl in an Ar (purity: 99.99%) atmosphere. It has been reported that inward grown δ-Ni_2Al_3 phase forms using the same pack cementation method at 620 °C[7,16]. Accordingly, the CeO_2-free and CeO_2-modified δ-Ni_2Al_3 coatings were prepared by aluminizing the electrodeposited Ni-CeO_2 and Ni films on Ni plate, respectively.

Afterwards, the aluminized specimens were oxidized in air at 1000 °C. Thermo gravimetric analyzer (TGA, Thermo Cahn 700) was used to measure the oxidation kinetics. After oxidation, the phases of the coatings were characterized using X-ray diffraction (XRD). The microstructures of the coatings and the oxide scales grown on the coatings were investigated using scanning electron microscopy (SEM) and energy dispersive spectroscopy (EDS).

2 Results and Discussion

2.1 Microstructure

Fig.1 shows the cross-sectional morphologies of the electrodeposited Ni and Ni-CeO_2 films on Ni plate (after etching in 4 vol% HNO_3+C_2H_5OH). The thicknesses of the electrodeposited films are ~10 μm. The co-deposited CeO_2 particles were exfoliated during etching, and consequently the original particle locations left the black holes in Ni-CeO_2 film (Fig.1b). It contains ~3.5 wt% CeO_2 in Ni-CeO_2 film, as revealed by the EDS analysis results. After aluminization, the cross-sectional morphology of the δ-Ni_2Al_3 coating formed on the Ni plate with a ~ 10 μm-thick Ni film is shown in Fig.2a. The aluminide coating is ~43 μm-thick. The CeO_2-modified δ-Ni_2Al_3 coating of similar thickness also formed on the Ni plate with Ni-CeO_2 film, as seen from Fig.2b. In fact, the δ-Ni_2Al_3 coatings without or with CeO_2 particles have a bi-layered structure. The outer layer (~30 μm-thick) is transformed from the electrodeposited Ni or Ni-CeO_2 film, while the inner layer is transformed from the underlying Ni substrate, as detailed in the earlier work [7]. The white particles in the magnified image of the A-framed zone in Fig.2b are the nanoparticles of CeO_2, which are randomly dispersed in the outer layer of the aluminide coating.

2.2 Oxidation

Fig.3a shows the isothermal oxidation kinetics of the CeO_2-free and CeO_2-modified δ-Ni_2Al_3 coatings for 20 h oxidation in air at 1000 °C. It demonstrates that the mass gain of the CeO_2-modified aluminide coating is lower than that of the

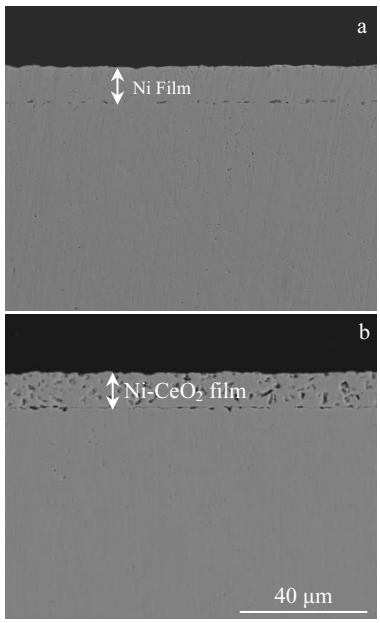

Fig.1 SEM morphologies of cross-section of the electrodeposited Ni (a) and Ni-CeO_2 (b) film on Ni plate (after etching in 4 vol% HNO_3+C_2H_5OH)

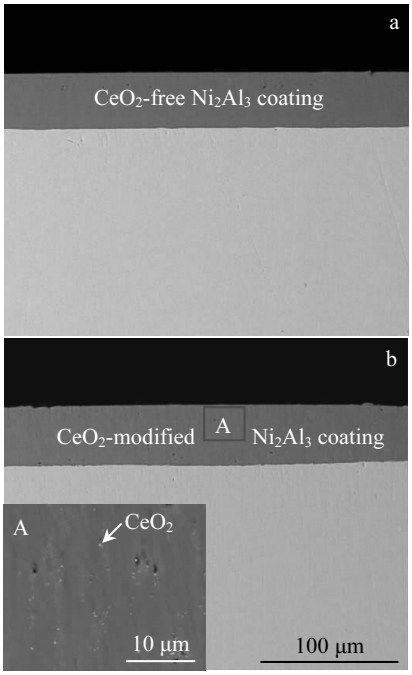

Fig.2 SEM morphologies of cross-section of the δ-Ni_2Al_3 coating on Ni plate, by aluminizing a ~10 μm-thick Ni film (a) and a ~10 μm-thick Ni-CeO_2 film (b) (the inset on the lower left is a magnified image of the A-framed zone in Fig.2b)

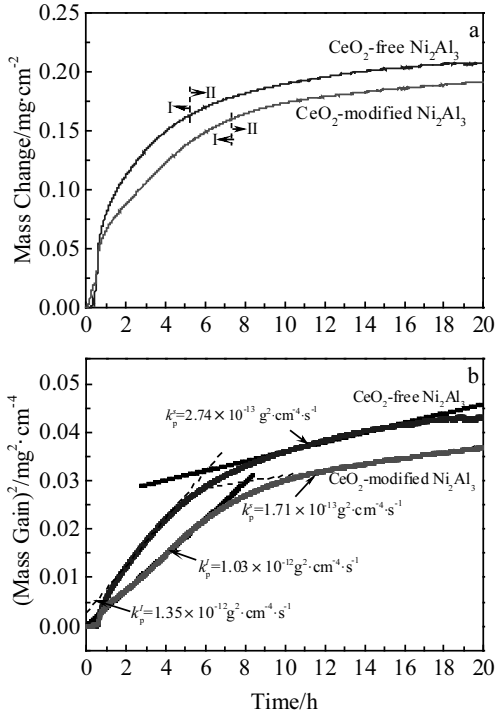

Fig.3 Isothermal oxidation kinetics (a) and the corresponding parabolic plots (b) of CeO_2-free and CeO_2-modified δ-Ni_2Al_3 coatings for 20 h oxidation in air at 1000 °C

CeO_2-free one. According to the difference of oxidation rate, the oxidation process of the CeO_2-free aluminide coating could be divided into two stages: initial stage (stage "I") with the faster oxidation rate and steady-state (stage "II") with a slower oxidation rate. The parabolic oxidation rate constants for different periods of the two aluminide coatings are clearly shown in the corresponding parabolic plots of Fig.3b. The oxidation of the CeO_2-free aluminide coating have two stages: stage "I" with a large parabolic oxidation rate constant k_p^I of ~1.35×10^{-12} $g^2\cdot cm^{-4}\cdot s^{-1}$ and stage "II" with a lower parabolic oxidation rate constant k_p^s of ~2.74×10^{-13} $g^2\cdot cm^{-4}\cdot s^{-1}$. The CeO_2-modified aluminide coating with respect to the CeO_2-free one have lower parabolic oxidation rate constants for both stage "I" and stage "II" (k_p^I is ~1.03×10^{-12} $g^2\cdot cm^{-4}\cdot s^{-1}$ and k_p^s is ~1.71×10^{-13} $g^2\cdot cm^{-4}\cdot s^{-1}$). It is considered that the transition from stage I to stage II corresponds to the formation of a continuous α-Al_2O_3 scale. From Fig.3a, it can be seen that the transition time to stage II for CeO_2-modified coating is later than that of the CeO_2-free coating.

The aluminide coatings after 20 h oxidation at 1000 °C were characterized using XRD and the results are presented in Fig.4. A protective scale of α-Al_2O_3 forms for the CeO_2-free aluminide coating (Fig.4a), while the alumina scale in both α and θ forms exists for the CeO_2-modified one (Fig.4b) after 20 h oxidation. Moreover, δ-Ni_2Al_3 completely degrades into Ni-rich β-NiAl phase ($Ni_{0.58}Al_{0.42}$) and Ni_3Al in the detected area for the CeO_2-free aluminide coating. However, only Ni-rich β-NiAl phase ($Ni_{0.58}Al_{0.42}$) is acquired for the CeO_2-modified aluminide

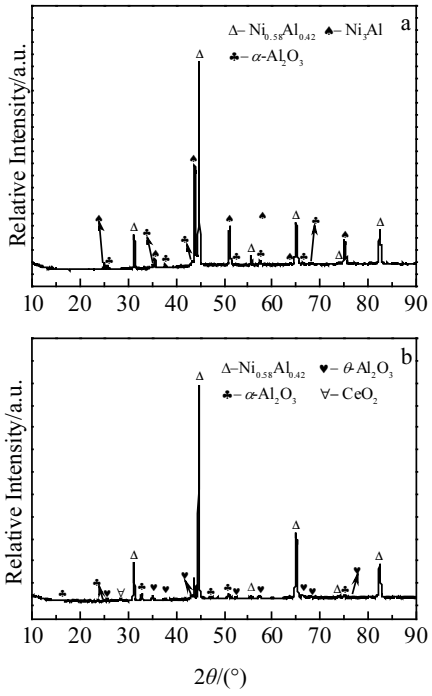

Fig.4 XRD patterns of CeO_2-free (a) and CeO_2-modified (b) δ-Ni_2Al_3 coatings after 20 h isothermal oxidation at 1000 °C

coating, as shown in Fig.4b. Fig.5 shows the SEM surface morphologies of the aluminide coatings after 20 h oxidation at 1000 °C. It reveals that a small amount of spallation occur on the surface of the CeO_2-free aluminide (Fig.5a). However, spallation of the CeO_2-modified aluminide coating is not observed after oxidation for 20 h, as shown in Fig.5b. From a magnified image of the surface alumina scale (Fig.5a′), it exhibits a fine whisker and blade-like configuration. After CeO_2 particles were added into the coating, the oxide scale on the surface could be divided into two areas: a blade-like area (A) and a smoother area (B), as presented in Fig.5b′. Pint et al [23] believe that these smoother areas correspond to the location of the doped rare-earth oxide particles.

SEM cross-sectional morphologies of both CeO_2-free and

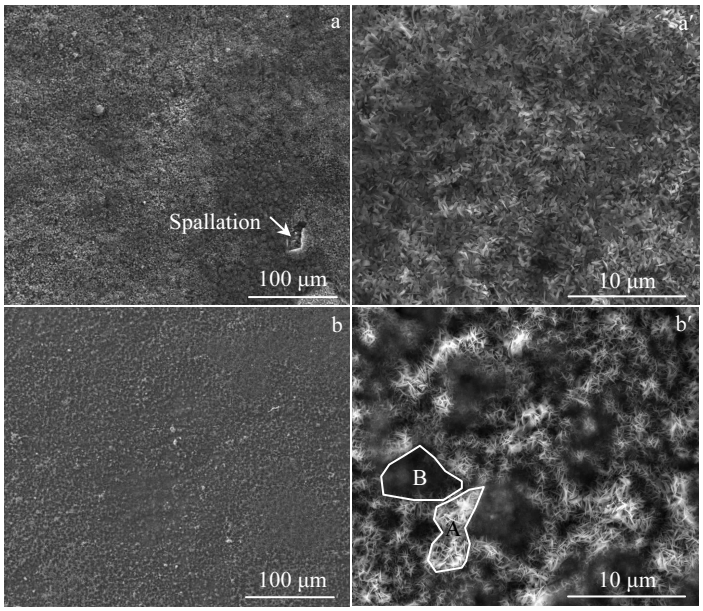

Fig.5 Surface morphologies of CeO_2-free (a) and CeO_2-modified (b) δ-Ni_2Al_3 coatings after 20 h isothermal oxidation at 1000 °C; (a′) and (b′) are the magnified images of the alumina scale in (a) and (b), respectively

CeO_2-modified coatings after oxidation are shown in Fig.6. It can be seen that the coatings degrade into two distinct layers after oxidation. The outer layer is Ni-rich β-NiAl and the inner layer is γ'-Ni_3Al on basis of the XRD and EDS analysis. Moreover, there are discontinuous γ'-Ni_3Al phases dispersing in the outer β-NiAl layer of the CeO_2-free aluminide coating (as arrowed in Fig.6a), which correspond to the rapid Al diffusion channels (the locations of grain boundaries). With respect to the CeO_2-free coating, the thinner alumina scale and the much thicker β-NiAl layer formed on the CeO_2-modified coating reveal that Al depletion within the CeO_2-modified coating is much lighter. Furthermore, cracking and spallation of the oxide scale occur on the CeO_2-free coating, while the CeO_2-modified coating exhibits better alumina adhesion. Small cavities are observed at the alumina/aluminide interface (as arrowed in Fig.6b). Besides, cavities are observed in the two aluminide coatings as well.

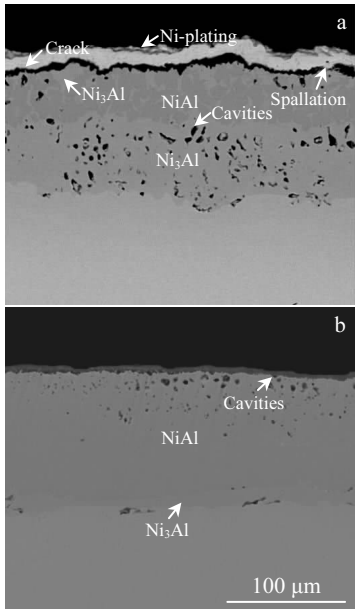

Fig.6 SEM morphologies of cross-section of CeO_2-free (a) and CeO_2-modified (b) δ-Ni_2Al_3 coatings after 20 h isothermal oxidation at 1000 °C

2.3 Discussion

The oxidation kinetics and XRD results of CeO_2-free and CeO_2-modified aluminide coatings show that the addition of CeO_2 delays the formation of a continuous α-Al_2O_3 scale and decreases the growth rate of alumina scale. Based on the earlier study, it is generally considered that there are four stages for the

transition of transient alumina to stable α-Al_2O_3 during oxidation [24]. At the initial stage of oxidation, transient alumina (such as γ, θ) forms (stage 1). Afterwards, α-Al_2O_3 nucleates at the interface of transient Al_2O_3/alloy matrix (stage 2). With the extension of time, α-Al_2O_3 transversely grows into a continuous layer (stage 3). Once a continuous α-Al_2O_3 layer forms, the oxidation rate of the aluminide coating would show a significant decrease, which corresponds to the change from stage "I" to stage "II" in oxidation kinetics (as shown in Fig.3). Finally, the residual transient Al_2O_3 completely transforms into α-Al_2O_3 (stage 4). From the above process, it can be seen that α-Al_2O_3 nucleates on the basis of transient Al_2O_3.

Many studies have shown that the addition of RE oxides greatly accelerates the transformation of θ-α phase compared with alloying and ion implantation [25], which might be relevant with the nucleation mechanism of α-Al_2O_3. If the nucleation mechanism of α-Al_2O_3 is diffusion nucleation, α-Al_2O_3 is easier to nucleate at the aggregation position of the anionic and cationic vacancies[26]. The addition of oxide particles induces a large number of particle/alloy interfaces, which are conducive to the condensation of vacancies and accordingly provide many heterogeneous nucleation points for α-Al_2O_3. However, this simple nucleation effect cannot totally explain the influence of oxide particle doping on phase transition of Al_2O_3. The doping ions' own chemical properties may have greater impact on the transition. Burtin et al[27,28] believe that the radius and valence of the doped ions are the key factors that affect the phase transition of transient Al_2O_3 to α-Al_2O_3. According to their model, the addition of CeO_2 particles would hinder the transition from transient Al_2O_3 to α-Al_2O_3 due to the large ionic radius and high valence of the rare earth element, thus delaying the formation of a continuous α-Al_2O_3 scale. At the same time, CeO_2 particles dissolved in alumina scale decompose and release Ce ions due to the higher surface energy of nanoparticles during oxidation[17]. The Ce ions prefer to diffuse outward along the grain boundaries because of the larger ionic radius with respect to Al ions. Consequently, the growth of both θ-Al_2O_3 and α-Al_2O_3 scale is suppressed by the absence of CeO_2 nanoparticles through inhabiting the outward diffusion of Al ions along the grain boundaries. As a result, the CeO_2-doped area (B in the Fig.5b′) exhibits a smoother surface morphology, while the area without CeO_2 doping remains the whisker- and blade-like configuration of θ-Al_2O_3. The effect of CeO_2 dispersion on the oxidation kinetics is a synergistic effect of the two points above. Although the formation of a continuous α-Al_2O_3 scale is delayed, the oxide scale of CeO_2-modified coating grows more slowly than that of CeO_2-free one.

In addition, the oxidation results also show that the CeO_2-modified coating exhibits better alumina adhesion compared with the CeO_2-free one. When the aluminide coatings are performed at high temperature, the degradation of coatings both arising from the outward diffusion to form alumina scale and the inward diffusion into the substrate occurs. The aluminide coatings in its δ phase would transform into Al-rich β phase at the onset of oxidation. The Kirkendall vacancies induced by the relatively higher diffusion rate of Al to Ni in Al-rich β-NiAl phase, together with the cationic vacancies, condense and then form cavities in the outer layer of the coating[29]. The vacancies prefer to condense at the high energy areas such as the interface of the alumina scale/aluminide coating and the interface between CeO_2 and aluminide. Scale spallation occurs when large-size cavities form at the scale/coating interface of the CeO_2-free coating (Fig.6a). While the CeO_2 particles are added into the aluminide coating, the presence of CeO_2 particles near interface could increase the sites for the condensation of vacancies and reduce the size of cavities at the interface (Fig.6b). Thus, the scale adhesion is greatly improved. Besides, the Kirkendall vacancies diffuse inward to the inner layer of the aluminide coating due to a relatively higher diffusion rate of Ni to Al in the Ni_3Al phase[30,31]. Accordingly, cavities also form in the inner layer of aluminide coating, which could be clearly seen in Fig.6a.

3 Conclusions

1) The addition of nanometer CeO_2 in aluminide coating of δ phase delays the formation of a continuous α-Al_2O_3 scale and decreases the growth rate of alumina scale during oxidation at 1000 °C.

2) The addition of nanometer CeO_2 in aluminide coating of δ phase improves the alumina scale adhesion due to the smaller cavities formed at the alumina scale/coating interface.

References

1 Nguyen T D, Peng X, Zhang J *et al. Surface and Coatings Technology*[J], 2017, 316: 226

2 Mollard M, Rannou B, Bouchaud B *et al. Corrosion Science*[J], 2013, 66: 118

3 Bai M, Sarakinou E, Chen Y *et al*. *Journal of the American Ceramic Society*[J], 2015, 98(12): 3639

4 Peng X, Clarke D R, Wang F. *Oxidation of Metals*[J], 2003, 60(3-4): 225

5 Pint B A, Martin J R, Hobbs L W. *Solid State Ionics*[J], 1995,78(1-2): 99

6 Li D, Guo H, Peng H *et al. Applied Surface Science*[J], 2013, 283: 513

7 Tan X, Peng X, Wang F. *Corrosion Science*[J], 2014, 85: 280

8 Pint B A, Haynes J A, Besmann T M. *Surface and Coatings Technology*[J], 2010, 204(20): 3287

9 Shirvani K, Firouzi S, Rashidghamat A. *Corrosion Science*[J], 2012 ,55: 378

10 Li B, Sun Z, Hou G *et al. Journal of Alloys and Compounds*[J], 2017, 692: 420

11 Xu J, Liu A, Wang Y *et al. Rare Metal Materials and Engineering* [J], 2016, 45(6): 1413

12 Zhou Z, Peng H, Zheng L *et al. Corrosion Science*[J], 2016, 105: 78

13 Zhan Q, Yang H G, Zhao W W *et al*. *Journal of Nuclear*

Materials[J], 2013, 442(1-3): 603
14 Hou P Y. *Materials Science Forum*[J], 2011, 696: 39
15 Hou P Y. *Journal of the American Ceramic Society*[J], 2003, 86(4): 660
16 Xu C, Peng X, Wang F. *Corrosion Science*[J], 2010, 52(3): 740
17 Peng X, Guan Y, Dong Z *et al. Corrosion Science*[J], 2011, 53(5): 1954
18 Pint B A, Martin J R, Hobbs LW. *Oxidation of Metals*[J], 1993, 39(3-4): 167
19 Wang X, Peng X, Tan X *et al. Scientific Reports*[J], 2016, 6: 511
20 Pint B A, Tortorelli P F, Wright I G. *Materials and Corrosion*[J], 1996, 47(12): 663
21 Hou P Y, Priimak K. *Oxidation of Metals*[J], 2005, 63(1-2): 113
22 Li Q, Peng X, Zhang J Q *et al. Corrosion Science*[J], 2010, 52(4): 1213
23 Pint B A, Alexander K B. *Fundamental Aspects of High Temperature Corrosion*[J], 1997, 145(6): 1819
24 Hou P Y. *Annual Review of Materials Research*[J], 2008, 38: 275
25 Huang Y, Peng X. *Corrosion Science*[J], 2016, 112: 226
26 Bagwell R B, Messing G L, Howell P R. *Journal of Materials Science*[J], 2001, 36(7): 1833
27 Burtin P, Brunelle J P, Pijolat M *et al. Applied Catalysis* [J], 1987, 34: 225
28 Burtin P, Brunelle J P, Pijolat M *et al. Applied Catalysis*[J], 1987, 34(1-2): 239
29 Paul A, Kodentsov A A, van Loo F J J. *Journal of Alloys and Compounds*[J], 2005, 403(1-2): 147
30 Cserháti C, Paul A, Kodentsov A A *et al. Intermetallics*[J], 2003, 11(4): 291
31 Chen G X, Wang D D, Zhang J M *et al. Physica B: Condensed Matter*[J], 2008, 403(19): 3538

CeO_2 改善低温渗铝涂层抗氧化性能的研究

谭晓晓

(上海工程技术大学，上海 201620)

摘　要：在 Ni 基体上电沉积纯 Ni 镀层和 Ni-CeO_2 复合镀层并对其进行 620 ℃低温渗铝，制备了无 CeO_2 和 CeO_2 改性的铝化物涂层。将以上 2 种涂层在 1000 ℃下氧化，研究 CeO_2 颗粒的加入对氧化膜的生长速率和粘附性能的影响。结果表明，在 δ-Ni_2Al_3 涂层中加入纳米 CeO_2 颗粒可以推迟一层完整 α-Al_2O_3 膜的形成时间，降低氧化膜的生长速率。此外，纳米 CeO_2 颗粒的加入提高了氧化膜的粘附性。原因是与没有 CeO_2 掺杂的涂层相比，CeO_2 改性铝化物涂层在氧化膜/涂层界面上形成的空洞尺寸较小。

关键词：铝化物涂层；氧化；包埋渗铝；活性元素效应

作者简介：谭晓晓，女，1988 年生，博士，讲师，上海工程技术大学材料工程学院，上海 201620，电话：021-67791247，E-mail: xxtan@sues.edu.cn